

Short Communication

Preparation of Electrostatic Spinning Composite Film Loaded with Polyvinylpyrrolidone for the Detection of Free Radicals in Polluted Air

Guoying Wang¹, Yanrong Liu¹, Qiuping Zhao^{1,*}, Xuefu Chen¹, Shengxue Hu², Lan Li¹, Xia Jiang¹, Chao Liu¹, Shiming Jia¹, Haoqi Tian¹, Yucan Dong¹, Peng Zhang¹, Hua Ma¹, Gaofeng Shi^{1,*}

¹ School of Petrochemical Engineering, Lanzhou University of Technology, Lanzhou, China

² PetroChina Fushun petrochemical Company Catalyst Plant, Fushun, China

*E-mail: gaofengshi_lzh@163.com, wanguoying@lut.cn

Received: 8 July 2018 / Accepted: 23 September 2018 / Published: 5 November 2018

An electrospinning system was used to elongate the prepared radical-scavenging antioxidant compounds into a fibrous-structured nanomaterial under the action of electrostatic force, and its structure was characterized by scanning electron microscopy. The trapping performance of the electrospun membrane was evaluated by comparing the sampling results of two membranes, and the integral peak areas were used for the detection of free radicals also obtained. The experimental results show that the electrospun membrane can effectively trap free radicals in polluted air, and the changes in the integral peak areas of free radicals are related to volatile organic compounds, particulate matters, sulphur dioxide, nitrogen dioxide, carbon monoxide, ozone, sampling time, temperature, and humidity. Subsequently, the nanomaterial was used for outfield sampling, and the sampling performance was measured using a fluorescence spectrophotometer.

Keywords: Air pollutants, Active molecules, Detection of free radicals, Electrospun membrane, Fluorescence spectrophotometer

1. INTRODUCTION

There are a large number of types of free radicals, such as hydroxyl, peroxy, alkoxy, nitroxide, and sulfate/sulfite free radicals, in the atmosphere. The short-lived, colourless, and tasteless free radicals at low concentrations and with strong oxidizing properties are not easily detected by the human body and can react with air pollutants in only a few seconds [1-3]. There are numerous types of free radicals in the atmosphere. Currently, the techniques used for detecting free radicals include ultraviolet-visible absorption spectroscopy (UV-vis), fluorescence methods, the electron spin

resonance spin-trapping technique, the laser-induced fluorescence (LIF) method, high-performance liquid chromatography (HPLC), and electrochemical methods. Sergej [4] used UV-vis absorption spectroscopy to study alkyl, vinyl, aryl and hydrogen peroxide free radicals in aqueous solution, as well as some related free radicals. ShotaIizumi [5] observed adenine free radicals in a low temperature argon matrix for the first time with UV-vis absorption spectroscopy. Zhang [6] developed a method for the quantitative detection of free radicals by fluorescence. In this method, the content of free radicals in aqueous solution was determined indirectly using the change in the fluorescence intensity of a capture agent before and after reacting with hydroxyl radicals. Harbour [7] studied the process of the UV photolysis of the adducts of OH and HO₂ radicals with nitrones in an aqueous hydrogen peroxide solution using the electron spin resonance technique. Matsumi [8] detected the tropospheric OH radicals using a laser-induced fluorescence instrument. In that method, the ambient air was expanded through a pinhole into a low-pressure fluorescent cell and then analysed. Koşar [9] used a modified HPLC post-column method to identify the effects of the reaction between free radicals and phytochemicals in complex mixtures. To study the effect of natural antioxidants on atmospheric free radicals, Wang [2] generated free radicals under laboratory conditions by burning tobacco to simulate the atmospheric environment.

In this paper, the electrospinning system was used to stretch a prepared antioxidant solution into a fibrous-structured nanomaterial under action of the electrostatic force, and the resultant structure was characterized by scanning electron microscopy (SEM). Subsequently, the nanomaterial was used for outfield sampling, and the sampling performance was measured using a fluorescence spectrophotometer. The trapping performance of the electrospun membrane was evaluated by comparing with the sampling result of a control membrane, and the change in free radicals was also obtained. This nanomaterial is lightweight and portable, and the active ingredient can stably exist on the membrane, so it can be carried on a drone for high-altitude sampling and can reflect the change in certain pollutants to some extent within a specified area.

2. EXPERIMENTAL

2.1 Materials and equipment

Polyvinylpyrrolidone (PVP) with an average molecular weight of 1,300,000 and methanol were purchased from Shanghai Macklin Biochemical Co., Ltd. and Cinc High Purity Solvents (Shanghai) Co., Ltd., respectively. The antioxidant compound was purchased from TCI (*Shanghai Development Co., Ltd.*). All of these chemicals were of analytical grade and could be used without further purification. The instruments and equipment used in this experiment included an 85-2 Constant Temperature Magnetic Stirrer (Guohua Electric Appliance Co., Ltd.), an ultrasonic cleaner (Ningbo Xinzi Biotechnology CO., LTD.), an SS-2533 electrospinning system (voltage: 220V/50Hz, current: 10 A, Beijing Ucalery Technology Development Co., Ltd.), a JSM-6701F cold field-emission scanning electron microscope (*Japan Electron Optics Laboratory Company*), a liquid chromatography (LC,), a fluorescence photometer (FL, LS-55, Perkin Elmer, USA), an intelligent medium-volume air sampler

for total suspended particulate (Wuhan Tianhong Instruments Co., Ltd.), and an On-line electronic sensors (Xianhehuanbao Instruments Co., Ltd.) for the determination of air pollutants.

2.2 Solution preparation

(1) Preparation of the electrospinning solution

First, the radical-scavenging antioxidant compounds (RSACs, mixtures, including hydroxyl benzoic acid, hydroxybenzoic acid glycoside and phenyl carboxylic acids) were extracted and purified. The preparation of fresh willow bark sample extracts was carried out using thermal reflux extract method. Fresh willow bark was comminuted, and each time, one kilogram of the fresh willow bark was immediately extracted in 10 L water/ methanol/sulphuric acid (35:55:10, v/v/v) by use of ultrasonic cell grinder and thermal reflux. Then the extracts were mixed together. After 60 minutes, the extract was concentrated in a vacuum to syrup, diluted and partitioned with ultrapure water, n-butyl alcohol, ethyl acetate, chloroform, and petroleum ether. Then the layers was filtered and dried by vacuum evaporation to afford a residue. Finally, the residues were subjected to testing the free radical activity respectively. The residue with high capacity for radical reactivity was screened and identified by LC and FL according to comparison with pure chemical. The RSACs with higher radical-scavenging capacity were selected to use in further experiments. Next, the radical-scavenging RSACs were mixed with PVP (6:100, m/m) and dissolved in methanol and water. The solution was stirred with a magnetic stirrer for 45 min at room temperature and was allowed to stand for 10 min. Finally, a uniform spinning solution was obtained and stored in a refrigerator for future use.

2.3 Electrospinning

The electrospinning system consisted of three parts: an injector, a rolling receiving device, and a high-voltage electrostatic field. The electrospinning experiments were performed at room temperature. The spinning solution obtained in the solution-preparation process (1) was placed in a 5 ml syringe, which was connected to a No. 21 stainless-steel needle with an inner diameter of 0.51 mm. The needle was connected to the positive electrode of a high-voltage power supply, and the negative electrode was connected to the receiving device. Subsequently, six sheets of glass-fibre-attachedaluminium foil were covered on the roller, and the electrospinning parameters were set as follows: spinning voltage: -2 kV to 8 kV; distance between the needle and the receiver: 16 cm; injection speed: 0.18 mm/min; translational displacement: 80 mm; and roller receiving speed: 40 r/min. The electrostatic spinning composite film was thus prepared in this manner.

2.4 Characterization

These active RSACs can react with hydroxyl radicals in the atmosphere to produce an adduct that can generate fluorescence signals.

Because the glass fibre membrane exhibits good air permeability, it can be used to capture the atmospheric particulates while also acting as a support material for the electrostatic spinning composite film. The outdoor sampling was performed with a glass fibre membrane covered with a nanofibre membrane. Before and after sampling, the aforementioned nanofibre membranes were cut into dimensions of approximately 3 mm in length and 3 mm in width, and their morphological structure was examined by SEM.

After sampling, the two membranes were crushed and dissolved in 15 ml of methanol, which was then sonicated for 10 min. The resulting filtrate was diluted to the mark of a 50 ml volumetric flask with deionised water and stored in a refrigerator for subsequent performance determination. The scanning range of the fluorescence emission photometer was set from 200 to 800 nm, the emission light wavelength was 350 nm, the scan speed was 200 nm/min, and the grating width was 10 nm.

2.5 Outfield sampling

The sampling site was selected as the 15th floor of the Complex Building, Lanzhou University of Technology, Gansu Province, China. Two samplers of the same model were placed in the same well-ventilated area, and two membranes were placed on the samplers. The same sampling time was used to perform the outfield sampling, and the environmental parameters were recorded. The sampling period was in late November, and the times were from 8:30 to 9:30 in the morning, from 14:00 to 15:00 in the afternoon and from 20:00 to 21:00 in the evening. The total volatile organic compounds (TVOCs), particulate matters (PM₁₀, PM_{2.5}), sulphur dioxide (SO₂), nitrogen dioxide (NO₂), carbon monoxide (CO), ozone (O₃), temperature, and humidity were monitored on-line at the interval time of 10 min in the nearby area for the assessment of environment parameters.

3. RESULTS AND DISCUSSION

The morphology of the electrostatic spinning composite film was characterized using SEM. Figure 1 shows the surface morphology of electrostatic spinning composite film. It can be seen that electrostatic spinning composite film tended not to restack with one another and enhancing the reaction surface area. The formed molecular clusters' size (coccoid) on the electrostatic spinning composite film ranged from hundred nanometers to several micrometers. The electrostatic spinning composite film's SEM (Fig. 1 a1, a2) images show a uniform topography, network-like structure. The formed porous and network-like structures could strengthen the effective surface and facilitate the reactions between RSACs and radicals in polluted air. The electrostatic spinning composite film could alter the surface property and preventing RSACs' agglomeration. Furthermore, the electrostatic spinning composite film can act as a platform for reactions between RSACs and radicals. The developed composite film can also strengthen the intensity of resistances to air shock. Figure 1 a1, b1, a2 and b2 show the SEM images of the electrostatic spinning composite film before and after sampling, respectively. The number of pixels in the SEM images in a1 and b1 are 2000, and the number of pixels

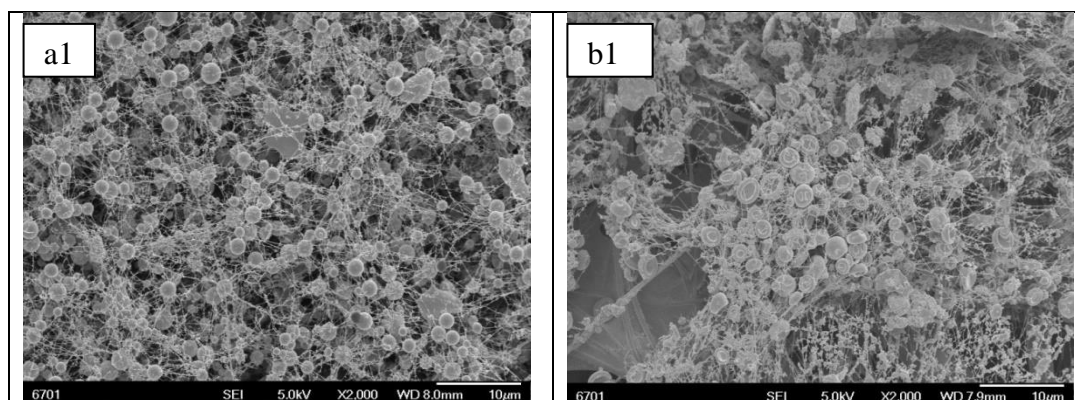
in the SEM images in a2 and b2 are 5000. According to the four images, we observed clearly structures' variation before and after reaction with radicals in polluted air.

During the preparation of electrostatic spinning composite film, methanol, active RSACs and the polymer are mixed in spinning solution. The characterization of the solution is identified and compared with standard molecules by liquid chromatography. The methanol evaporated during the electrospinning process, and the PVP polymer was stretched into a filamentous shape under the electrostatic force. As a result, the spherical RSACs shown in a1 and a2 were associated with the active material, and the oblate spheroids in b1 and b2 revealed the products obtained after the reaction between the active RSACs and hydroxyl radicals. The PVP formed an ideal network structure, and the generated space was relatively large. In the process, the active RSACs were not integrated with the PVP but instead were uniformly dispersed within the fibrous structure formed by the electrospinning of the polymer.

The structure of the active RSACs changed considerably after sampling. The original spherical shape converted into an oblate spheroid, and the diameter increased to some extent. We observed a large number of small particles attached to the nanofibres after sampling. The average diameter of the nanofibres was 100 nm. On the other hand, as shown in b1 and b2, the diameter of the glass fibres of the glass fibre membrane was approximately 600 nm, considerably larger than the diameter of the fibres formed from PVP. Therefore, the nanofibres formed by electrospinning exhibited a larger specific surface area than did the glass fibres and could trap more pollutant molecules.

The control membrane was formed via direct application of the active RSACs solution to the glass fibre membrane and was easily scattered by the wind during sampling, affecting the experimental results. On the other hand, the nanofibrous structure formed by electrospinning could affix the active RSACs firmly to the substrate.

Furthermore, the prepared electrospun membrane have a certain strength to resist the air stream damage, the obtained active molecular membranes can be carried by unmanned aerial vehicle for the detection of spatial (Altitude gradient change 100 m - 3000 m) and temporal variation of free radicals in polluted air, which can effectively trap free radicals from the atmosphere, and the obtained results also reflected the relationships between atmospheric free radicals and the factors (such as TVOCs, PM₁₀, PM_{2.5}, SO₂, NO₂, CO, O₃, temperature and humidity).



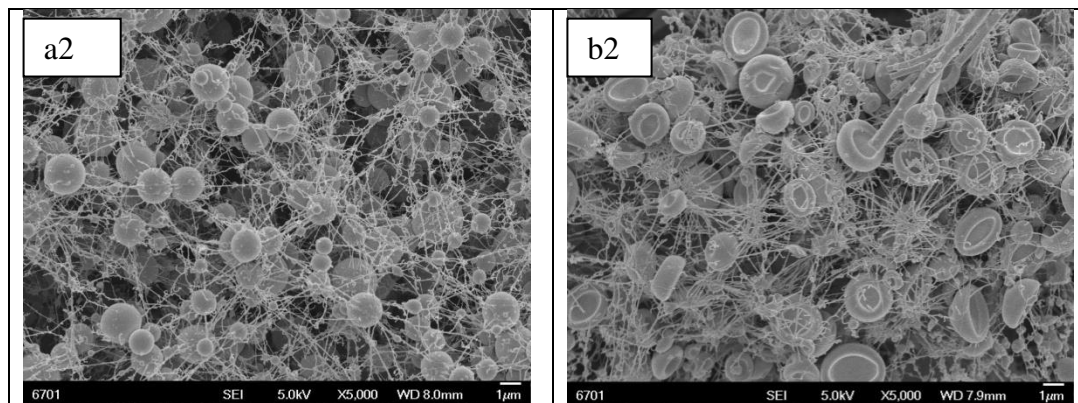
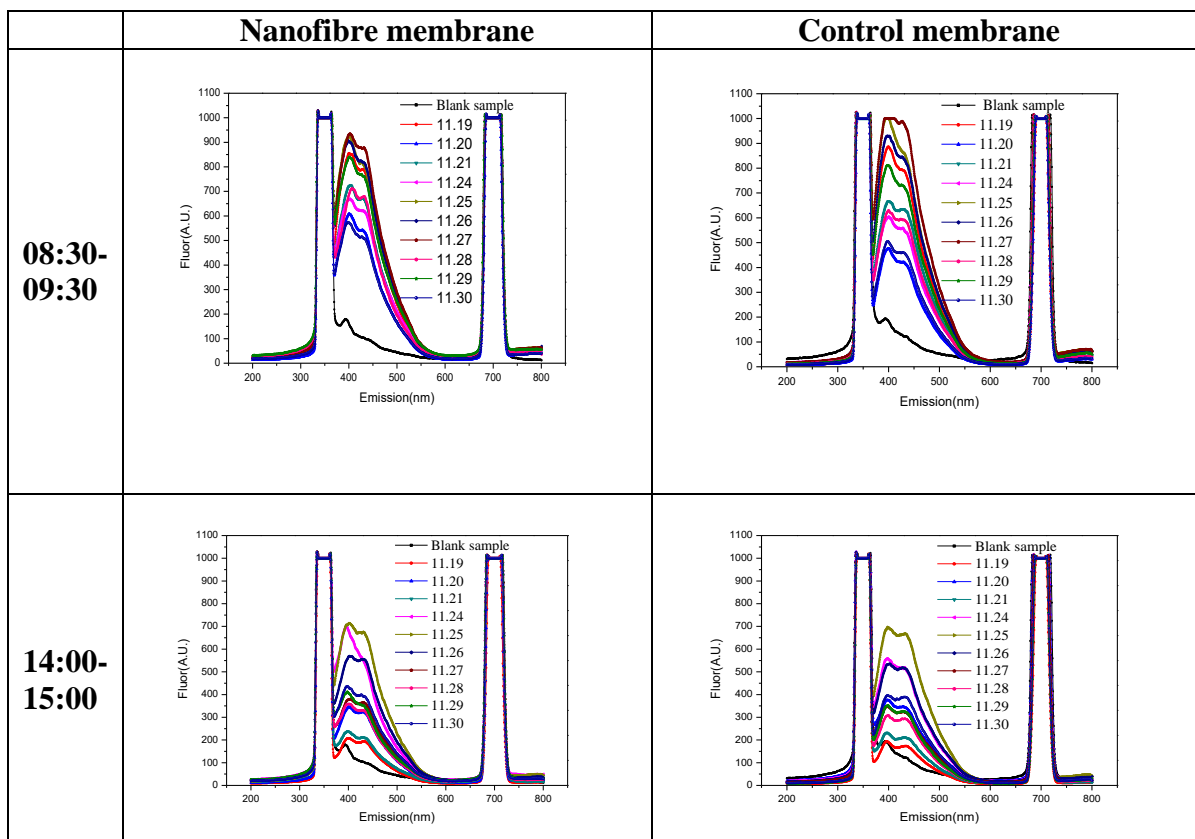


Figure 1. SEM characterization of electrostatic spinning composite film before and after sampling

The spectrum was obtained from the electrostatic spinning composite film before sampling. As revealed in the spectrum, the fluorescence signal intensity of the electrostatic spinning composite film at 430 nm was very weak before sampling, which indicated that the composition of the electrostatic spinning composite film produced little fluorescence signal.



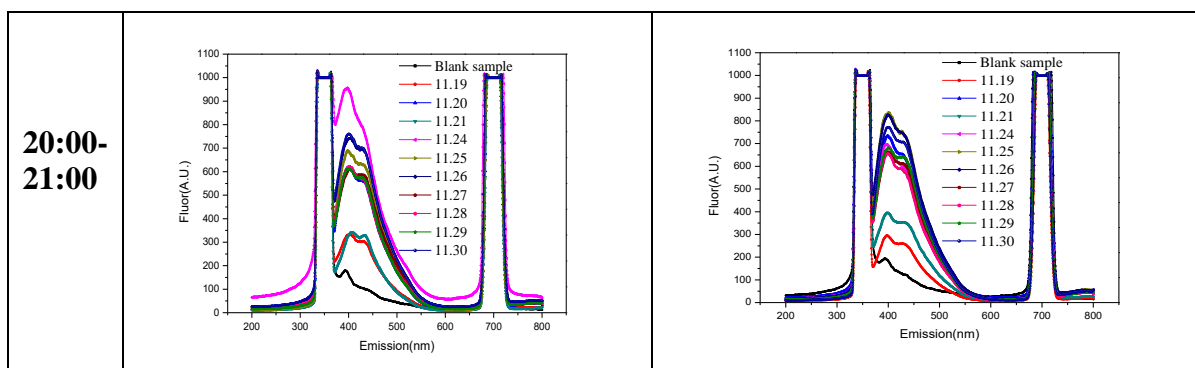


Figure 2. The fluorescence spectra of the electrostatic spinning composite film and the control membrane before and after sampling.

The spectra were obtained from the electrostatic spinning composite film after samplings, and the signal intensity was significantly increased after sampling, suggesting that the active RSACs on the electrostatic spinning composite film reacted with the atmospheric free radicals to produce an adduct that could generate a fluorescence signal. The photo-electrochemical sensor for determination of hydroquinone [10], electrochemical oxidation of benzoic acid derivatives [11], electrochemical sensor for assaying of drug based on benzoic acid molecule [12], detection of radicals with reaction with benzoic acid [13], and simple electrochemical method for the determination of hydroxyl radical [14] were have been developed earlier based on electrochemical mechanisms. The flavonoids, phenolic acids and its' derivatives related liquid samples have been researched based on the developed electrochemical methods. However, for the gas samples, few methods have been developed for the detection of radicals in polluted air. Especially for the electronic methods, weak signal changes in gas sample could not be detected by electrochemical method. Therefore, an electrostatic spinning composite film was prepared for the trapping of radicals in polluted air. Furthermore, an adduct having fluorescence properties would form in the composite film after sampling form polluted air. Figure 2 shows the fluorescence spectra of the electrostatic spinning composite film and the control membrane before and after sampling. The blank samples in the plots represented to the two membranes before sampling. As presented in the plots, nearly no fluorescence signal was found at the emission wavelength of 430 nm before sampling, while the signals of both membranes at 430 nm after 10 d of sampling were substantially enhanced [6]. Overall, the changes in the amount of free radicals detected by the two membranes over 10 d were essentially consistent with those obtained during a single day. Both morning and evening fluorescence signals were stronger than the afternoon signals. As shown from the trends of the spectra of the two membranes in the morning, the variation in the fluorescence signal at 430 nm within 10 d was not very great, but the signal intensity in the morning was relatively strong when compared to the overall signals in the afternoon and in the evening. As viewed from the trends of the spectra of the two membranes in the afternoon, the changes in the fluorescence signal intensity within 10 d were concentrated between 300 nm and 400 nm and were relatively stable. As indicated by the trends of the spectra of the two membranes in the evening, the changes in the fluorescence signal intensity within 10 d were concentrated between 550 nm and 750 nm. From the analysis results, we concluded that the free radical contents of this area in the morning and evening

were higher than that in the afternoon. After comparison and validation with the control membrane, we concluded that the electrostatic spinning composite film can effectively trap pollutants from the atmospheric environment, and different active RSACs can be selected as trapping agents to capture different pollutants from the atmosphere.

Table 1S (SUPPORTING MATERIAL) shows the environmental parameters (TVOCs, PM₁₀, PM_{2.5}, SO₂, NO₂, CO, O₃, temperature and humidity) and the sampling periods in the morning (8:30 - 9:30), afternoon (14:00 - 15:00), and evening (20:00 - 21:00) during the 10 d of sampling. As shown in the table, TVOCs range from 144.2 to 637 $\mu\text{g}/\text{m}^3$ during the 10 d sampling period, the concentrations of TVOCs in the morning were generally higher than those in afternoon. PM₁₀ ranges from 67 to 218 $\mu\text{g}/\text{m}^3$, PM_{2.5} ranges from 25 to 115 $\mu\text{g}/\text{m}^3$, SO₂ ranges from 14 to 45 $\mu\text{g}/\text{m}^3$, NO₂ ranges from 5 to 154 $\mu\text{g}/\text{m}^3$, CO ranges from 0.364 to 4.468 mg/m^3 , O₃ ranges from 4 to 135 $\mu\text{g}/\text{m}^3$, temperature ranges from 0.4 to 10 °C, and humidity range from 22% to 66% during the 10 d sampling period. The temperatures in the morning and evening during the 10 d sampling period were generally lower than those in the afternoon, and the humidity in the morning and evening was generally higher than that in the afternoon. The morning sampling covered the period when the concentration of traffic pollutants was high, and various pollutants might be emitted by different industries during the evening sampling period. TVOCs, O₃, CO, NO₂, low temperatures, high humidity, and the sampling period might be the source of the changes in the fluorescence signals presented in Figure 2.

4. CONCLUSIONS

In this work, an active molecular membrane that trapped air pollution molecules was primarily prepared by an electrospinning system. The obtained active molecular membranes were used for outfield sampling, and the sampling performance was determined by fluorescence spectroscopy. The analysis of the measured results demonstrated that this electrostatic spinning composite film can effectively trap free radicals from the atmosphere, and the obtained results also reflected the changes in atmospheric free radicals and the factors (such as TVOCs, PM₁₀, PM_{2.5}, SO₂, NO₂, CO, O₃, temperature and humidity) that affect these changes in free radical concentrations. Furthermore, the obtained active molecular membranes can be carried by unmanned aerial vehicle for the detection of spatial (Altitude gradient change 100 m - 3000 m) and temporal variation of free radicals in polluted air.

ACKNOWLEDGMENTS:

This work was supported by the National Key Research and Development Program of China (2016YFC0202900), National Natural Science Foundation of China (21567015), Natural Science Foundation of Gansu Province (17JR5RA109), Gansu Provincial Party Committee Young Creative Talents (Ganzutongzi [2017]121).

References

1. S. Gligorovski, R. Strekowski and S.J. Barbati, *Chemical Reviews*, 24 (2015) 13051.
2. G.Y. Wang, X.M. Lei, G.F. Shi, F.Y. Li and T.C. Guo, *Oxid. Commun.*, 39 (2016) 2904.
3. G.Y. Wang, S.M. Jia, X.L. Niu, H.Q. Tian, Y.R. Liu, X.F. Chen, L. Li, Y.H. Zhang and G. F. Shi, *Sci. Total environ.*, 609 (2017) 1103.
4. S. Naumov and C.V. Sonntag, *J. Phys. Org. Chem.*, 7 (2011) 600-602.
5. S. Iizumi, S. Ninomiya, M. Sekine and M. Nakata, *J. Mol. Struct.*, 1025 (2012) 43-47.
6. X. Zhang, F. Si and K.L.Y an, CN103149188, (2013).
7. J.R. Harbour, V. Chow and J.R. Bolton, *Can. J. Chem.*, 20 (1974) 3549.
8. Y. Matsumi, M. Kono, T. Ichikawa, K. Takahashi and Y. Kondo, *B. Chem. Soc. Jpn.*, 75 (2002) 711-717.
9. M. Koşar, D. Dorman, K. Başer and R. Hiltunen, *Chromatographia*, 60 (2004) 635-638.
10. H.Y. Wu, J.C. Hu, H. Li and H.X. Li, *Sensor Actuat. B-Chem.*, 182 (2013) 802-808.
11. B. Louhichi, N. Bensalash and A. Gadri, *Chem. Eng. Technol.*, 29 (2006) 944-950.
12. B. Nigovic and J. Spajic, *Talanta*, 86 (2011) 393-399.
13. G.W. Klein, K. Bhatla, V. Madhavan and R.H. Schuler, *The J. Phys. Chem.*, 79 (1975) 1767-1774.
14. H. Zou, C. Tai, X.X. Gu and R.H. Zhu, *Anal. Bioanal. Chem.*, 373 (2002) 111-115.

© 2018 The Authors. Published by ESG (www.electrochemsci.org). This article is an open access article distributed under the terms and conditions of the Creative Commons Attribution license (<http://creativecommons.org/licenses/by/4.0/>).

SUPPORTING MATERIAL

Table 1S. The environmental parameters (TVOCs, PM₁₀, PM_{2.5}, SO₂, NO₂, CO, O₃, temperature and humidity) and the sampling periods

Monitoring Date	Monitoring times	TVOC (µg/m ³)	PM ₁₀ (µg/m ³)	PM _{2.5} (µg/m ³)	SO ₂ (µg/m ³)	NO ₂ (µg/m ³)	CO (mg/m ³)	O ₃ (µg/m ³)	Temperature (°C)	Humidity (%)
2017-11-19	08:30	500.0	127	57	27	62	1.586	8	1.0	58.0
	08:40	482.8	119	60	28	58	1.594	9	1.0	58.0
	08:50	501.3	180	79	28	67	1.926	7	1.0	58.0
	09:00	510.8	218	107	32	67	2.044	7	0.4	57.6
	09:10	455.5	195	96	30	65	2.024	7	1.0	57.0
	09:20	440.5	203	104	34	69	2.274	8	1.0	56.0
	09:30	498.8	194	86	27	91	2.198	8	1.0	66.0
2017-11-19	14:00	250.0	98	33	21	8	0.468	87	8.2	30.4
	14:10	277.8	75	25	18	5	0.364	86	8.2	30.6
	14:20	210.3	75	27	20	11	0.434	83	8.0	30.6
	14:30	285.3	90	30	20	8	0.476	83	8.0	30.6
	14:40	281.0	86	30	20	16	0.468	81	8.4	30.4
	14:50	365.8	94	33	20	22	0.462	77	8.6	31.0
	15:00	268.8	79	28	20	13	0.474	84	8.0	31.4
2017-11-19	20:00	477.5	71	26	20	32	0.658	72	4.0	36.8
	20:10	347.5	75	26	17	34	0.558	67	4.0	36.4
	20:20	277.0	88	30	16	50	0.674	51	4.0	37.0
	20:30	272.3	98	34	16	63	0.966	41	4.0	37.4

	20:40	378.3	88	30	17	58	0.850	44	4.0	37.2
	20:50	375.5	81	28	16	64	0.860	37	4.0	37.4
	21:00	479.3	98	35	17	74	1.084	24	4.0	38.8
	08:30	509.3	130	59	17	55	1.584	11	1.0	52.8
	08:40	490.5	138	69	18	65	1.838	6	1.0	52.8
	08:50	496.8	161	65	19	65	1.520	8	1.0	52.0
2017-11-20	09:00	492.5	115	56	20	61	1.530	14	1.0	51.6
	09:10	453.3	144	59	20	63	1.482	10	1.0	50.6
	09:20	481.3	177	65	20	62	1.744	15	1.0	49.6
	09:30	521.5	153	63	23	69	2.322	10	1.0	49.2
	14:00	480.3	111	52	26	106	1.686	17	6.0	35.6
	14:10	435.0	130	57	24	104	1.816	20	6.0	36.4
	14:20	441.0	117	56	24	102	1.640	24	7.0	35.8
2017-11-20	14:30	465.3	107	53	22	106	1.672	22	6.6	35.8
	14:40	440.8	105	49	23	95	1.576	29	6.0	36.0
	14:50	434.0	105	49	25	98	1.492	27	6.0	35.2
	15:00	416.0	94	45	24	89	1.396	35	6.4	34.8
	20:00	509.5	163	82	19	102	1.656	6	3.0	44.0
	20:10	513.8	151	73	18	95	1.450	5	3.0	44.0
	20:20	474.8	151	68	21	92	1.398	8	2.0	44.0
2017-11-20	20:30	511.3	121	62	19	84	1.356	11	2.0	44.2
	20:40	481.3	130	62	18	85	1.408	9	2.0	44.6
	20:50	503.5	119	61	18	89	1.420	11	2.0	44.8
	21:00	528.9	144	65	18	91	1.296	8	2.0	45.0
	08:30	423.0	127	50	24	63	1.354	14	1.0	43.2
	08:40	400.5	113	45	24	69	1.324	10	1.0	43.6
	08:50	422.0	113	47	24	71	1.294	9	1.0	43.2
2017-11-21	09:00	492.5	125	49	25	71	1.370	11	1.0	43.4
	09:10	540.3	127	50	24	71	1.364	11	1.0	42.8
	09:20	494.0	104	46	26	78	1.388	8	1.0	42.2
	09:30	472.5	138	54	26	78	1.430	7	1.0	42.0
	14:00	291.8	79	26	30	20	0.548	80	4.4	28.6
	14:10	345.8	77	26	28	17	0.470	76	5.0	28.2
	14:20	343.8	88	28	29	28	0.582	67	5.0	28.6
2017-11-21	14:30	300.3	85	30	31	24	0.572	71	4.4	28.4
	14:40	341.3	79	26	31	15	0.552	84	4.2	28.2
	14:50	372.3	77	26	29	12	0.522	87	4.4	27.8
	15:00	344.5	77	27	28	21	0.552	80	5.0	28.2
	20:00	339.0	106	35	19	59	0.788	45	1.0	37.0
	20:10	402.3	79	32	19	58	0.820	44	1.0	37.0
	20:20	464.5	92	33	18	59	0.756	47	1.0	36.6
2017-11-21	20:30	314.8	92	29	18	56	0.830	48	1.0	36.8
	20:40	256.0	79	27	19	35	0.730	67	1.0	36.0
	20:50	293.8	67	25	18	49	0.840	51	1.0	36.8
	21:00	262.8	77	27	19	33	0.676	69	1.0	36.6
2017-11-24	08:30	245.5	161	83	25	76	1.974	5	1.0	52.4
	08:40	253.3	159	83	25	79	2.200	7	1.0	51.8

	08:50	232.5	132	79	24	75	1.984	7	1.0	51.8
	09:00	362.0	165	86	25	69	1.938	9	1.0	51.4
	09:10	264.5	180	88	27	73	2.086	10	1.0	50.6
	09:20	241.5	170	90	26	80	2.104	6	1.0	49.8
	09:30	194.8	168	90	27	83	2.406	7	1.0	49.0
	14:00	224.3	136	71	33	71	1.212	89	9.0	26.4
	14:10	178.0	128	71	31	71	1.102	88	9.0	26.2
	14:20	191.0	115	66	33	73	1.148	93	9.0	26.2
2017-11-24	14:30	218.3	119	65	33	64	1.098	99	9.4	24.6
	14:40	151.8	117	64	30	71	1.064	93	9.8	24.4
	14:50	218.0	113	63	29	78	1.164	89	9.4	23.8
	15:00	220.8	153	85	23	154	1.964	34	9.0	26.0
	20:00	162.3	146	57	22	89	1.228	14	2.0	31.8
	20:10	182.3	98	49	20	89	1.242	10	2.0	31.6
	20:20	194.8	115	52	21	90	1.212	8	2.0	31.4
2017-11-24	20:30	243.8	94	49	21	84	1.210	13	2.0	31.0
	20:40	258.3	96	48	20	81	1.146	17	2.0	30.4
	20:50	179.3	128	57	20	100	1.384	5	1.4	31.6
	21:00	162.3	157	62	21	100	1.480	6	1.0	32.4
	08:30	247.3	136	66	30	71	1.932	4	1.0	45.8
	08:40	221.8	159	73	29	64	1.862	8	1.0	46.2
	08:50	236.5	124	71	31	66	1.880	9	1.0	45.6
2017-11-25	09:00	239.5	180	78	30	72	1.840	5	1.0	44.6
	09:10	296.8	161	75	30	76	1.790	6	1.0	43.4
	09:20	256.8	132	69	30	74	1.896	8	1.0	41.8
	09:30	276.8	130	70	29	74	1.832	7	1.0	40.2
	14:00	174.4	133	67	42	75	1.35	86	9.0	22.0
	14:10	169.3	137	69	39	87	1.408	80	9.0	22.4
	14:20	159.4	133	67	40	82	1.462	87	9.0	23.0
2017-11-25	14:30	218.0	140	71	40	102	1.692	84	9.0	22.8
	14:40	209.0	151	79	33	140	2.110	56	9.0	23.0
	14:50	199.5	148	76	36	130	1.978	59	9.6	22.2
	15:00	192.5	150	78	32	137	1.950	42	10.0	23.0
	20:00	167.0	172	92	22	118	2.276	7	2.0	35.2
	20:10	144.2	142	73	20	105	1.576	7	1.4	34.2
	20:20	155.5	150	78	21	112	1.700	8	1.0	34.2
2017-11-25	20:30	199.5	127	63	19	92	1.370	12	1.0	33.8
	20:40	196.8	114	55	21	84	1.166	13	1.0	32.6
	20:50	206.3	140	73	19	95	1.426	7	1.0	33.8
	21:00	240.3	130	65	19	95	1.500	6	1.0	34.0
	08:30	234.5	174	93	17	80	2.068	7	1.0	50.6
	08:40	228.3	189	103	22	76	3.238	5	1.0	50.8
	08:50	254.0	184	99	20	80	2.528	6	1.0	50.4
2017-11-26	09:00	262.3	186	101	20	81	2.464	5	1.0	50.0
	09:10	235.8	183	99	22	83	2.520	6	1.0	49.2
	09:20	233.3	207	115	29	86	3.626	8	1.0	48.2
	09:30	237.3	206	114	27	91	3.156	7	1.0	46.8

2017-11-26	14:00	211.3	184	99	45	117	1.740	133	9.0	27.4
	14:10	235.8	174	93	40	103	1.586	135	9.0	26.4
	14:20	252.5	170	91	37	96	1.554	132	9.0	25.0
	14:30	268.5	171	92	34	112	1.686	121	9.0	24.8
	14:40	260.5	178	96	31	126	2.254	116	9.0	25.0
	14:50	280.3	175	94	29	118	1.820	108	8.0	25.2
	15:00	235.8	156	81	28	121	1.738	85	9.0	24.2
2017-11-26	20:00	577.8	148	77	17	96	1.428	11	2.0	33.6
	20:10	555.0	142	73	20	95	1.348	16	2.0	33.4
	20:20	531.8	147	76	19	103	1.544	7	2.0	34.4
	20:30	492.5	144	74	21	87	1.432	15	2.0	33.8
	20:40	556.3	147	76	22	86	1.502	11	2.0	33.6
	20:50	530.0	146	75	20	101	1.718	8	2.0	34.6
	21:00	537.0	145	75	19	107	1.684	7	2.0	35.2
2017-11-27	08:30	391.8	174	93	25	87	2.124	4	1.0	50.8
	08:40	388.8	176	95	24	80	2.198	4	1.0	51.0
	08:50	420.5	163	86	23	83	2.234	5	1.0	50.6
	09:00	480.5	178	96	22	91	2.378	6	1.0	50.0
	09:10	474.3	175	94	22	89	2.126	8	1.0	49.4
	09:20	413.8	185	100	24	94	2.388	8	1.0	48.6
	09:30	395.0	188	102	31	89	4.468	6	1.0	48.0
2017-11-27	14:00	184.8	143	74	34	69	1.358	57	9.0	35.4
	14:10	186.0	137	69	32	59	1.266	62	9.0	36.6
	14:20	211.5	133	67	34	59	1.222	64	8.6	37.6
	14:30	183.5	129	65	33	42	1.078	79	8.0	38.2
	14:40	158.3	134	67	30	65	1.150	63	8.0	37.4
	14:50	203.3	133	67	31	68	1.114	59	8.6	37.8
	15:00	320.0	133	67	30	58	1.056	65	9.0	37.4
2017-11-27	20:00	324.3	159	84	19	106	1.654	14	2.0	45.8
	20:10	423.0	167	89	19	112	1.676	9	2.0	46.8
	20:20	425.5	164	87	19	107	1.710	11	2.0	47.2
	20:30	388.0	169	90	20	107	1.656	11	2.0	47.0
	20:40	400.0	191	104	21	109	1.882	9	2.0	47.4
	20:50	416.5	185	100	19	110	1.862	7	2.0	48.2
	21:00	369.5	175	95	20	108	1.708	8	1.4	48.0
2017-11-28	08:30	339.8	89	39	18	57	1.030	19	1.0	44.0
	08:40	308.5	88	39	19	53	0.914	21	1.0	42.4
	08:50	287.5	96	43	17	64	1.042	12	1.0	42.8
	09:00	253.5	109	52	16	73	1.234	8	1.0	43.0
	09:10	238.5	107	51	14	77	1.172	8	1.0	42.8
	09:20	252.8	105	49	16	78	1.220	8	1.0	42.0
	09:30	240.3	108	51	17	77	1.214	9	1.0	41.6
2017-11-28	14:00	226.3	89	39	36	54	0.816	45	5.0	28.2
	14:10	213.5	89	39	39	46	0.734	46	5.0	29.0
	14:20	232.0	84	36	39	61	0.836	39	5.0	29.4
	14:30	195.8	88	38	38	53	0.871	43	5.0	29.3
	14:40	202.3	94	42	37	81	1.109	33	5.0	30.7
	14:50	168.5	104	49	35	89	1.384	30	5.2	31.0

	15:00	151.0	109	52	36	87	1.264	29	5.6	30.6
	20:00	358.0	133	68	21	101	1.618	7	1.0	38.6
	20:10	364.5	128	64	21	98	1.532	5	1.0	38.6
	20:20	383.0	127	64	21	92	1.508	4	1.0	38.6
2017-11-28	20:30	336.3	131	66	26	96	1.624	4	1.0	38.6
	20:40	344.3	135	68	26	87	1.890	7	1.0	39.0
	20:50	348.5	178	97	29	94	1.958	8	1.0	39.2
	21:00	326.5	140	72	30	86	1.930	4	1.0	39.6
	08:30	351.3	133	67	16	74	1.724	8	1.0	51.4
	08:40	401.3	142	73	15	76	1.838	4	1.0	51.6
	08:50	398.3	137	70	18	80	1.822	6	1.0	51.4
2017-11-29	09:00	407.8	140	72	17	76	1.882	10	1.0	51.2
	09:10	325.5	175	94	24	87	3.274	7	1.0	51.0
	09:20	296.8	176	94	24	89	3.014	7	1.0	50.8
	09:30	320.0	169	90	21	89	2.320	8	1.0	49.8
	14:00	191.0	98	44	36	61	1.068	59	8.4	24.6
	14:10	217.0	103	48	30	81	1.110	50	7.4	26.4
	14:20	276.0	98	44	33	63	1.012	64	7.6	26.0
2017-11-29	14:30	262.7	99	45	31	63	0.970	62	8.0	25.4
	14:40	279.3	99	45	29	63	0.968	62	8.0	25.4
	14:50	308.5	95	43	25	81	0.954	46	8.0	25.2
	15:00	241.5	96	44	27	68	1.002	55	8.0	24.8
	20:00	222.0	98	45	22	73	0.892	16	2.0	33.0
	20:10	237.5	100	45	19	74	0.854	12	2.0	33.4
	20:20	213.5	96	43	21	82	0.962	9	2.0	33.2
2017-11-29	20:30	251.3	117	57	20	84	1.108	9	1.0	33.8
	20:40	272.3	109	52	21	86	1.092	7	1.0	34.0
	20:50	292.5	114	54	19	93	1.270	7	1.0	35.4
	21:00	276.0	106	50	20	86	1.168	8	1.0	35.8
	08:30	253.8	112	53	15	70	1.684	6	1.0	50.6
	08:40	236.5	114	55	15	67	1.598	5	1.0	50.6
	08:50	208.0	112	53	15	65	1.780	6	1.0	49.8
2017-11-30	09:00	220.8	116	56	15	66	1.698	7	1.0	49.6
	09:10	210.8	113	54	15	65	1.468	9	1.0	48.8
	09:20	225.3	119	58	19	70	2.114	8	1.0	47.8
	09:30	240.8	118	57	17	67	1.732	7	1.0	46.8
	14:00	174.0	93	41	27	43	0.798	124	8.0	24.6
	14:10	181.5	95	43	26	58	0.812	116	8.0	24.8
	14:20	207.5	99	45	25	75	1.072	105	8.0	24.8
2017-11-30	14:30	249.5	105	49	22	98	1.346	79	7.8	25.8
	14:40	205.5	106	49	23	108	1.428	72	7.0	27.0
	14:50	210.5	106	50	23	108	1.516	60	7.0	27.0
	15:00	197.5	105	49	22	108	1.440	47	7.0	27.0
	20:00	592.0	128	64	19	108	1.468	8	1.0	39.8
2017-11-30	20:10	637.0	129	65	18	100	1.376	7	1.0	40.0
	20:20	561.5	131	66	20	104	1.400	8	1.0	40.2
	20:30	544.0	127	63	22	108	1.470	4	1.0	40.6

20:40	548.0	133	67	22	100	1.540	8	1.0	40.8
20:50	528.5	136	69	17	106	1.638	5	1.0	42.2
21:00	535.5	121	59	18	105	1.340	8	1.0	42.0
